Radiation Physics and Chemistry 167 (2020) 108235

Contents lists available at ScienceDirect

Radiation Physics and Chemistry

journal homepage: www.elsevier.com/locate/radphyschem

Low cost electron irradiator using $^{90}Sr + ^{90}Y$ sources

Rogério M.V. Silva[a], Walmir Belinato[b], William S. Santos[c,d,e], Luiza F. Souza[f], Ana P. Perini[c,e], Lucio P. Neves[c,e], Divanizia N. Souza[f,*]

[a] Instituto do Câncer do Ceará, Fortaleza, CE, Brazil
[b] Departamento de Ensino, Instituto Federal de Educação, Ciência e Tecnologia da Bahia, Vitória da Conquista, BA, Brazil
[c] Instituto de Física, Universidade Federal de Uberlândia, Uberlândia, MG, Brazil
[d] Instituto de Pesquisas Energéticas e Nucleares, Comissão Nacional de Energia Nuclear (IPEN-CNEN/SP), São Paulo, SP, Brazil
[e] Programa de Pós-Graduação em Engenharia Biomédica, Faculdade de Engenharia Elétrica, Universidade Federal de Uberlândia, MG, Brazil
[f] Departamento de Física, Universidade Federal de Sergipe-UFS, São Cristóvão, SE, Brazil

ARTICLE INFO

Keywords:
Irradiator
Low cost
Electron
Pellets

ABSTRACT

In beta therapy, β particles from $^{90}Sr + ^{90}Y$ are used for the prevention and treatment of ophthalmological and dermatological diseases. For such purposes, the radiation dose is deposited by planar and concave applicators positioned on the region to be treated. Although this therapy is effective on the diseases, several complications have been reported, making these types of radioactive applicators obsolete in current clinical practice. This paper proposes a methodology to prepare and evaluate the safety of a research irradiator that re-purposes and adapts dermatologic and ophthalmic $^{90}Sr + ^{90}Y$ applicators. The irradiator was constructed using low cost materials and three applicator sources. The sources are positioned at the center and the upper end of acrylic rectangular prisms. Radiochromic film was used to obtain the dose distribution on the sample holder surface. Pellets of aluminum oxide doped with carbon (Al_2O_3:C) were used to evaluate the reproducibility of the irradiator. The MCNPX Monte Carlo code was used for the evaluation of safety conditions. The irradiator exhibits good reproducibility of irradiation of dosimeters in pellet form and is safe to handle.

1. Introduction

Brachytherapy envolving $^{90}Sr + ^{90}Y$ sources are employed to prevent and treat diseases in the eyes and skin with β particles. For this purpose, the applicators, with concave or planar radioactive surfaces, are utilized to deposit the dose on the surface to be treated. The main diseases threated with this therapyare the pterygium and keloids.

Pterygium is an ophthalmic disease characterized by a wing-like fibrovascular form, located on the conjunctiva and cornea (Altinkaynak et al., 2014). For the treatment, applicators containing $^{90}Sr + ^{90}Y$ sources are used on the eye surface. Besides the positive results from this treatment, several complications have been reported in the literature, such as corneal or scleral necrosis and endophthalmitis, reducing the use of these radioactive sources (Mackenzie et al., 1991; Willner et al., 2001).

Another common type of therapy using applicators containing $^{90}Sr + ^{90}Y$ sources is radiotherapy for the treatment of keloids (Froelich et al., 2007). Normally, the applicator is positioned in contact with the lesion, but besides the proeminent results, linear accelerators are usually employed nowdays. These devices are equipped with many different configurations and electron beams with different energies. In addition, images of the patient may be acquired using computed tomography (CT) or magnetic resonance (MR). With this information, the behavior of the electron beam can be simulated to choose the most suitable energy for each specific lesion.

For these reasons, several medical facilities worldwide have unutilized their sources, which can be a radiation protection problem, considering that ^{90}Sr has a half-life of approximately 28 years. On the other hand, many research centers are developing new dosimeters or investigating the action of this type of ionizing radiation in many organisms/materials; these researchers need to buy expensive irradiators for their facilities. Thus, an irradiator system that exploits these unused radioactive sources could reuse the applicators and minimize the costs of purchasing irradiators containing this type of source. The system would be required to present safe conditions for handling and a high reproducibility for the exposure of samples.

Therefore, the present work proposes a methodology of preparation, adaptation and safety evaluation for the construction of a low-cost research irradiator suitable for ophthalmic and dermatological applicators containing $^{90}Sr + ^{90}Y$ sources.

* Corresponding author.
E-mail addresses: lucio.neves@ufu.br (L.P. Neves), divanizi@ufs.br (D.N. Souza).

https://doi.org/10.1016/j.radphyschem.2019.03.039
Received 7 November 2018; Received in revised form 24 March 2019; Accepted 26 March 2019
Available online 29 March 2019
0969-806X/

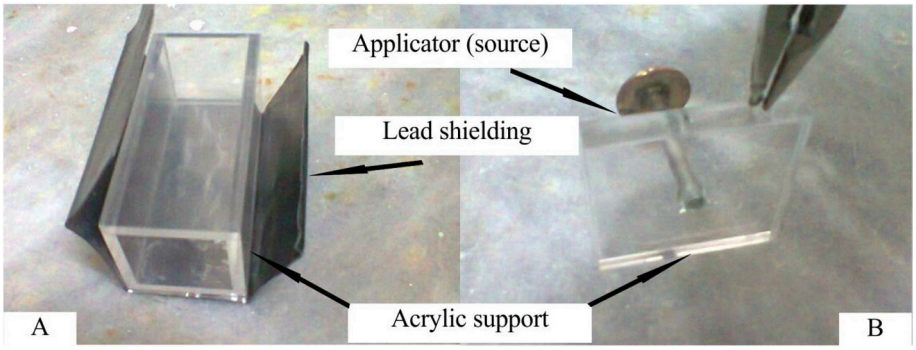

Fig. 1. a) Prism being covered with lead; b) source position and fixing procedure.

2. Materials and methods

2.1. Irradiator design

The irradiator prototype, named SAMARA, was constructed using polymethyl methacrylate (PMMA) 2.5 cm thick with rectangular external dimensions of 25 cm × 30 cm × 15 cm. Supports shaped as prisms were constructed to hold the applicators in an elevated position relative to a sample holder (Fig. 1A). The parts were fixed using acrylic glue. The irradiator prototype contained three sources, two concave and one planar that were fixed at the support, also made of acrylic (Fig. 1B). To prevent bremsstrahlung leakage, after assembly all parts were externally covered by a double lead layer (4 mm) that was fixed using Araldite adhesive. The configuration of the irradiator guaranteed that samples of 1.0 mm or more thick could be irradiated with a source surface distance of 3.0 mm. Fig. 1 shows the procedure to cover the prism and the applicator being positioned on the support.

To construct irradiation boxes, the supports with the applicators fixed at the central point were positioned at the upper part of the prisms. A T-shaped sample holder was fixed at the bottom of the main box. The upper part of sample holder has a cavity with dimensions of 225 mm^2 by 1 mm deep. In this cavity, samples can be irradiated in powder or pellet form. This part is removable, allowing proper cleaning procedures. Fig. 2 shows an irradiation box and the complete irradiator with its respective dimensions.

All applicators selected to construct the irradiator were manufactured by Amersham Health (Buckinghamshire, UK). Although some these applicators had been in use over 40 years, their external structures remained intact with no visible damage on their surfaces. The data on the applicators selected are shown in Table 1.

In these applicators, the radioactive ^{90}Sr material is embedded in silver and sealed with a stainless steel window to attenuate low-energy beta radiation. Fig. 3A and B shows the configuration (side view) of planar and concave applicators and the position of the ^{90}Sr inside the applicator, respectively.

The planar applicator has a thick support and a 0.05 mm stainless steel filter; the concave one has a 0.1 mm stainless steel filter and a radius of curvature of 10 mm. These intrinsic source configuration characteristics (spatial distribution) inside the encapsulation make these applicators an excellent option to evaluate the effects of electron radiation on small quantities of material.

2.2. Determining the dose surface using radiochromic film

Dosimetric studies using EBT radiochromic films allow us to estimate doses in two-dimensions in several clinical situations (Wilcox and Daskalov, 2007; Su et al., 2007). When exposed in regions of high dose gradient such as in therapeutic electron beams, these films exhibit a very accurate dosimetric response, making them a suitable tool where it is desired to know the planar behavior of doses (Su et al., 2007). Thus, pieces of Gafchromic™ EBT3 films (ISP, Wayne, NJ) were used to obtain the dose distribution on the sample holder surfaces.

Three irradiations were performed for each sample holder and for each selected exposure time (1, 2, 5 and 10 min). After the irradiation procedure, the EBT3 films were scanned in an Epson model 10000XL Scanner. The images were converted to dose maps using an RGB multichannel algorithm in Film QAPro software (Ashland ISP Advanced Materials, NJ, USA). These analyses allowed to identify the region of greatest dose uniformity on the sample-holder surface, and to estimate the dose rates.

2.3. Determining the dose rate using optically stimulated luminescence (OSL) dosimetry

OSL dosimetry has been included in many dosimetry procedures because of its fast readout and the possibility of re-reading from same exposure (Akselrod and McKeever, 1999; Yukihara and McKeever, 2008). To simulate the irradiation of materials in pellet form and verify the reproducibility of the exposures, pellets of aluminum oxide doped with carbon (Al_2O_3:C) 5.0 mm in diameter and 1.0 mm thick, were

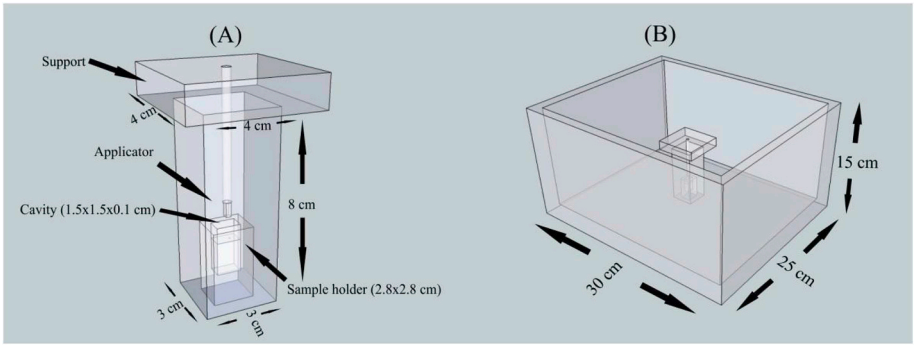

Fig. 2. Irradiator design: A) Irradiation box; B) Complete irradiator.

Table 1
Information on the applicators selected for irradiator.

Set number (sample holder and source)	Applicator type	Serial number	Nominal activity (MBq)	Calibration date (from manufacturer)
1	Ophthalmic (concave)	SIA6-1522	370	27.11.1973
2	Ophthalmic (concave)	SIQ6-9737	740	14.01.1992
3	Dermatological (planar)	SIA5-1520	74	27.11.1973

placed in the center of the sample holders and irradiated for different time periods (1. 2, 3 and 5 min).

The OSL measurements were performed using an OSL – DEN-PE reader, model DOIN-L001, equipped with blue and green LEDs, manufactured by the *Federal University of Pernambuco* (UFPE, Brazil) and a Logan model SAD-2000 data acquisition system. Nine dosimeters were used and three irradiations were performed for each exposure time and for each set (sample holder and source). Because the OSL response of these dosimeters was known from a previous calibration, with a reference source, it was possible to evaluate the dose rates of the three sources used in the irradiator. After each cycle of irradiation/measurement, the dosimeters were thermally treated at 400 °C for 1 h for subsequent reuse. Fig. 4A and B shows the film being positioned on the sample holder surface for irradiation and the irradiator with source being positioned for the pellet exposure, respectively.

The variability of a series of numbers can be measured by the coefficient of variation (c_v), independently of the unit used for the numbers (Abdi, 2010). To evaluate the reproducibility of the system for irradiations of samples in the pellet form, the c_v values were evaluated from three measurements (time of irradiation of 2 min) based on the OSL response. For these evaluations equation (1) was used:

$$c_v = \frac{S}{M}. 100 \quad (1)$$

where S is the standard deviation and M is the mean of the results.

2.4. Calibration set-up

For the film calibration, the methodology described by Barouky et al. (2011) was followed. Five pieces of film were irradiated with different doses (0.3, 0.5, 1, 3 and 5 Gy) and an additional film was kept separate with no irradiation to check the background, after 24 h from exposure. The irradiations were performed in a Varian (Palo Alto, CA) Clinac IX series linear accelerator. The set-up mounting guaranteed that each piece of the film was positioned in the reference depth for the selected energy of a 6 MeV electron beam. Although this energy is higher than the maximum energy emitted by a $^{90}Sr + ^{90}Y$ source, differences higher than 5% in the responses of the film, when irradiated with therapeutic electron beams, are not expected (Su et al., 2017).

For this calibration, a water phantom (acrylic box with dimensions of 37 × 37 × 37 cm^3 and 10-mm-thick) filled with distilled water was used. A 10 × 10 cm^2 electron applicator was adopted with a source-to-surface distance of 100 cm. The pieces of film (15 × 15 cm^2) were positioned vertically in the phantom and they were irradiated at the maximum dose depth. The films were scanned and their images exported to film QA PRO software to plot the calibration curve based on dose values obtained from the planning system. The absorbed dose results obtained from the irradiations performed with the linear accelerator were compared with those calculated with the Eclipse Treatment Planning System (Varian Medical Systems, Palo Alto, California) using the Generalized Gaussian Pencil Beam algorithm. The comparison was employed to validate the film calibration results.

For OSL dosimetry, the calibration curve (OSL response as a function of absorbed dose) was obtained using a $^{90}Sr + ^{90}Y$ clinical applicator from the calibration laboratory at the Instituto de Pesquisas Energéticas e Nucleares - IPEN - São Paulo-SP, manufactured by Atlantic Research Corporation, model B-1 S/N 233 (0.40 Gy/s, 2013), calibrated at the primary standard laboratory of the National Institute of Standards and Technology (NIST). Three irradiations were performed for each dosimeter with doses of 1, 2, 5, 7 and 12 Gy, using a source distance of 11 cm. The results from the OSL curve (integration area) were recorded to obtain the calibration curve. The OSL measurements were performed using an OSL–DEN-PE reader and a Logan model SAD-2000 data acquisition system.

2.5. Safety evaluation

To verify the safety of the irradiator and to evaluate the level of

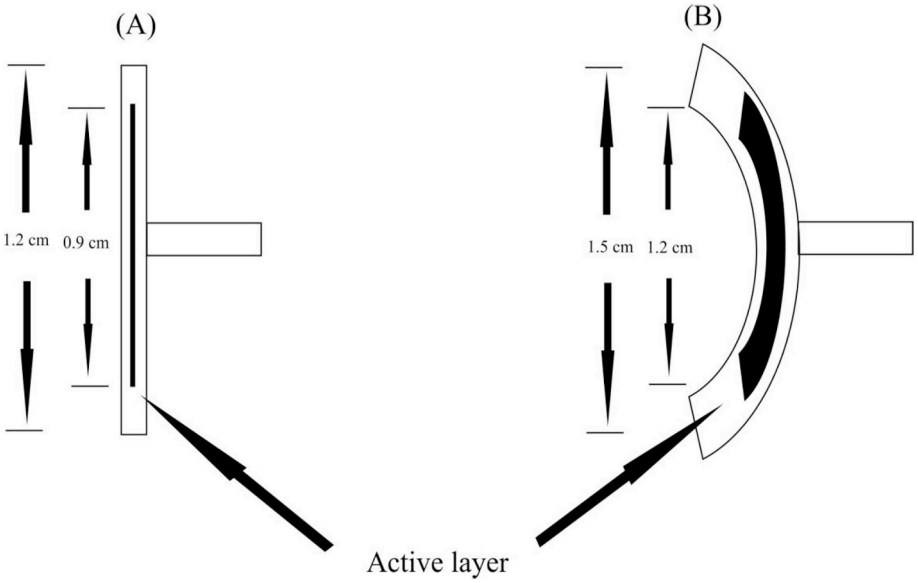

Fig. 3. A) Side view of planar applicator; B) Side view of concave applicator and respective dimensions based on Amersham catalog.

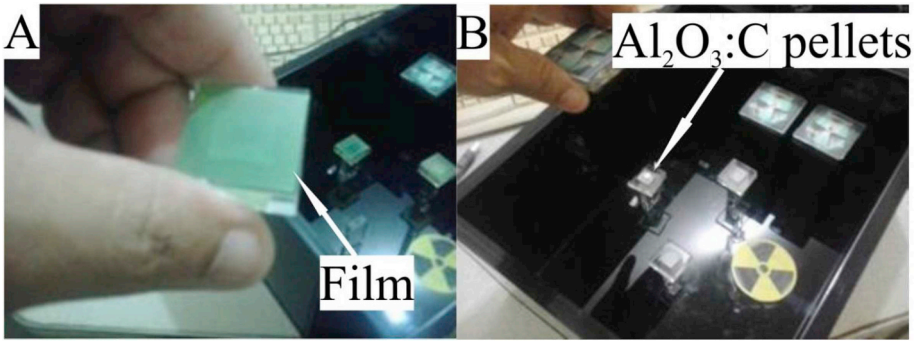

Fig. 4. SAMARA irradiator: A) Films being positioned on the sample-holder surface; and B) irradiation procedure for a sample in pellet form.

radiation exposure to which users were subjected during its handling, the procedure for placement and removal of samples was simulated using the MCNPX (version 2.7.0) radiation transport code. This code simulates the transport and interaction of electrons, photons and neutrons with matter in arbitrary three-dimensional geometries (Briesmeister, 2000; Santos et al., 2013).

The users of the simulator were considered Individuals Occupationally Exposed (IOE) and the dose limits for these IOE were considered (ICRP, 2007). For this reason, the user was simulated with a dosimeter positioned at the left side of the thorax to estimate the personal dose equivalent $H_p(10)$ in accordance with the ICRU (1993) methodology. The body of the user was represented by the FASH virtual anthropomorphic phantom (Cassola et al., 2010). The distance between the surface of the irradiator and the dosimeter in the simulation was approximately 44 cm. The ion chamber RADCAL, model 20X6-6, with an active volume of 6 cm^3 was used to determine the experimental dose values in the external wall surface of the irradiator. The results from experimental measurements were used to determine the conversion factor (CF), as presented in equation (2).

$$CF = \frac{rate\left(\frac{\mu Sv}{min}\right)}{*F8\ tally\left(\frac{MeV}{Particle}\right)} \tag{2}$$

The ion chamber was simulated in the scenario by a half sphere (detector B, Fig. 5A) positioned in the same region of the experimental measurements.

In Fig. 5A, detector A represents the volume used to estimate the personal dose equivalent $Hp_{(10)}$. The red point in Fig. 5C shows the position of detector B (Fig. 5A) used to validate the scenario.

The energy spectrum of the $^{90}Sr + ^{90}Y$ source was generated by a DEXRAX 32 decay data extractor (Eckerman et al., 1993). The radionuclides ^{90}Sr and ^{90}Y have half-lives $T_{1/2} = 28.64$ years and $T_{1/2} = 64.10$ h with maximum decay energies $\beta_{max} = 0.54$ MeV and $\beta_{max} = 2.28$ MeV, respectively. Due to the stainless-steel window, the maximum energy of the emerging β particles is typically about 2 MeV (Deasy and Soares, 1994). However, in this work we have chosen to assume that in the stable state, equilibrium is obtained in the population of electrons, and the energetic distribution of the ^{90}Sr and ^{90}Y is evenly distributed. Fig. 6 shows the normalized energy spectrum of emission probabilities used for the modeled source.

Including all steps related to the simulation, equation (3) describes the procedure to obtain the dose rate in a dosimeter positioned on the thorax and in the main organs of the user.

$$Dose\ rate = *F8\ tally\left(\frac{MeV}{particle}\right) \times CF\left(\frac{\mu Sv}{min} \cdot \frac{particle}{MeV}\right) \tag{3}$$

where *F8 tally is the Monte Carlo result and CF is the calibration factor, obtained from experimental measurements. The values and methodologies described in the ICRP (2007) were used to determine the personal dose equivalent, $H_p(10)$, and the organ doses. The determination of $H_p(10)$ was calculated using equation (4).

$$H_p(10) = Dose\ rate\left(\frac{\mu Sv}{min}\right) \times\ manipulation\ time\ (min) \tag{4}$$

In addition, the values of $H_p(10)$ and the sum of the dose values in the considered organs (effective dose), also obtained during the manipulation, were compared. The effective doses on organs were obtained using equation (5).

$$E = \sum_T w_T . H_T \tag{5}$$

where w_T is the weighting factor for each tissue considered and H_T is the equivalent dose to that tissue. In the evaluation of safety conditions, only photons were considered (weighting factor for γ radiation, w_R, is 1).

3. Results and discussion

3.1. Irradiator assembly

The assembly of the irradiator was very simple and we used only low-cost materials; however, attention is necessary to correctly localize the applicators in the irradiation set. To decrease the uncertainties of source position and optimize the maximum dose region in the center of the sample holder, the assembly procedure should avoid any slack on the rods of the applicators.

Although not described explicitly in the materials and methods section, all safety equipment important for handling a radiation source such as gloves, safety glasses, and a personal dosimeter must be used during the construction. It is also recommended that the procedure of fixing the applicators in the support be rehearsed using an object similar to the applicator. This practice may optimize the procedure of installing the real applicator, minimizing errors and the exposition time.

3.2. Gafchromic films results

The results obtained with radiochromic films allowed determining the optimal positioning of the sources relative to the sample holders and to estimate the dose rates. Fig. 7 shows a dose isomap, obtained with the film positioned on the sample holder surface of source 1 (set 1), after an irradiation time of 2 min. The highlighted square corresponds to the sample holder area.

For the set 1, the highlighted region (yellow circle) selected for dosimeter placement presented a mean absorbed dose rate of 21.65 mGy/s, for the second film irradiation. The differences between the three irradiations, performed for the three sets, were within 3%. It can be observed in the highlighted region that small changes in the sample position may promote different dose rates, reducing the reproducibility of the irradiation conditions considerably. To optimize this behavior, filters can be added on the applicator surface to decrease

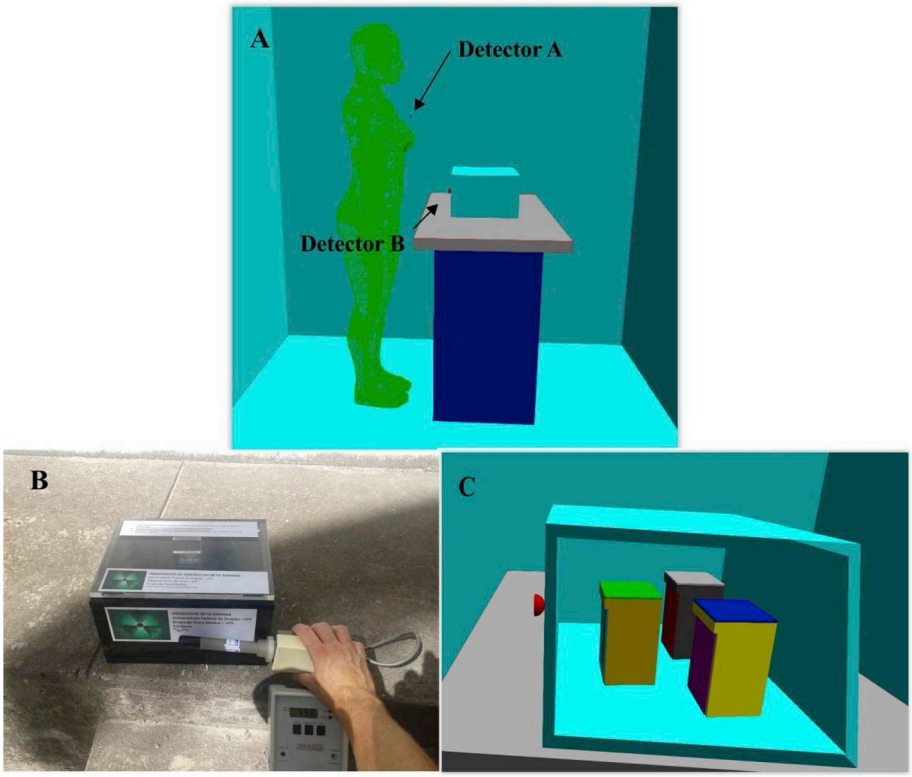

Fig. 5. A) Virtual scenario used in the MCNPX simulation, in a general view; B) the experimental procedure to obtain the exposure rate; C) side view of the irradiator and three internal sources.

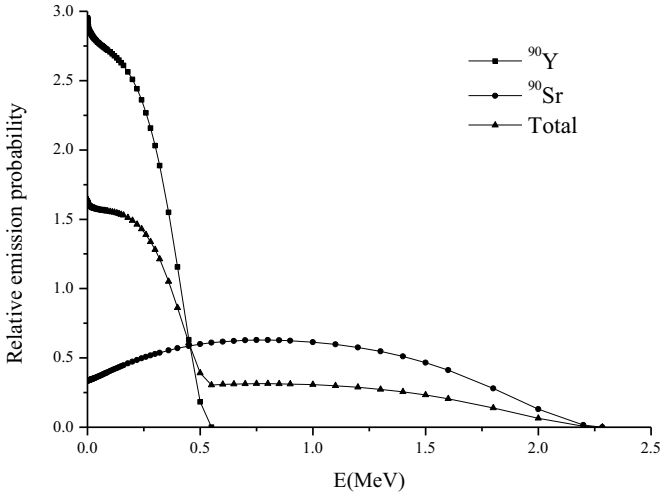

Fig. 6. ^{90}Sr + ^{90}Y spectrum used in MCNPX code.

the dose gradient. Table 2 summarizes the results obtained from the films. The values are mean dose values based on three measurements obtained on the yellow highlight circle in Fig. 7, for each individual set.

Considering the intrinsic characteristics of the applicators, related to dose distribution, it is essential for users to know the source isomap doses. For this reason, it is recommended that images of the three isomaps to be fixed on the irradiator. When a user performs an irradiation with powder or gel samples, the isomap dose profile should be consulted for better placement of the target material on the sample holder. Any asymmetries identified in the isomaps may be related to the damage of the applicators, possibly caused by mechanical shocks to their surfaces over time.

For this study, the central region of the sample holders (circle highlighted in Fig. 7) was selected for the OSL dosimeters, and all irradiator calibration procedures were performed for this area.

3.3. OSL dosimeters results

The major problem in determining the dose rates for electron beams from ^{90}Sr + ^{90}Y is the uncertainty associated with the obtained values. The highest dose gradient on the surface, and small differences in the placement of the dosimeters between irradiations, can increase the discrepancies between the measured doses values. This fact was verified, and the size of the sample holder was optimized to decrease movement of the irradiated material. Other reasons for the high uncertainty were proposed in the study of Antonio et al. (2014); they suggested that procedures to clean the surfaces of holder applicators cause inhomogeneities on their surfaces, causing differences in the mean dose rates. They also presented a system for postal dosimetry of ophthalmologic and dermatologic applicators, using two different techniques (OSL and TL dosimetry). A more recent certificate of calibration of the applicators used in the present work was obtained by this postal system (Antonio et al., 2014).

The mean dose rates obtained from OSL results for sets 1, 2 and 3 (sample holder and source) and the results presented by Antonio et al. (2014) for these sources are shown in Table 3.

Using the postal calibration results as a reference, the highest and lowest variations were 13.1% and 4.2%, for sets 2 and 1, respectively. This difference can be associated with small changes in the arrangement of the irradiator.

It seems reasonable to compare the results from different methodologies of irradiation; however, for the present study this type of comparison is beyond the objectives of this work. The use of different dosimetric techniques will lead to different sources of uncertainties, such as the angular and energy dependence, as well as the sizes and detector's materials. This may yield different results, which must be carefully evaluated. For this reason, we assume that the most

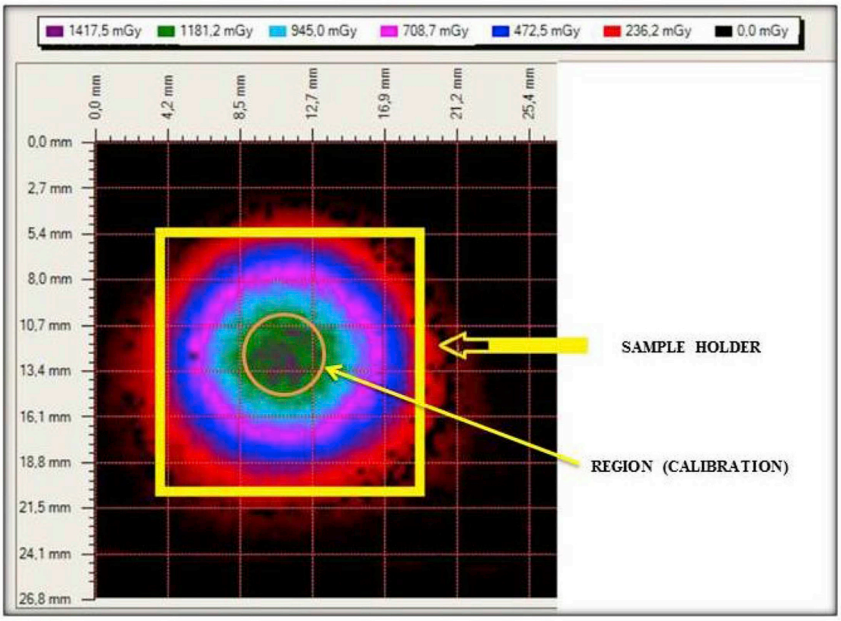

Fig. 7. Dose distribution on the sample-holder surface, set 1, 2 min exposure – second irradiation.

Table 2
Mean dose values obtained with Gafchromic film on region central of the sample holders.

Set number (sample holder and source)	Applicator (serial number)	Dose rate in mGy/s Highlight circle (± Standard deviation)
1	SIA6-1522	19.5 ± 3.1
2	SIQ6-9737	7.2 ± 1.5
3	SIA5-1520	13.8 ± 2.1

Table 3
Absorbed dose rates from OSL (SAMARA) and postal calibration.

Set number (sample holder and source)	Applicator (serial number)	Mean value of dose rate (mGy/s)	
		SAMARA OSL Results	Postal calibration[a]
1	SIA6-1522	13.9 ± 3.2	14.6 ± 4.4
2	SIQ6-9737	5.3 ± 2.3	6.1 ± 2.6
3	SIA5-1520	12.2 ± 3.4	11.7 ± 3.5

[a] Values on April, 2014 obtained from data originally supplied by the postal system.

Table 4
OSL results for 3 measures performed in set 1.

Dosimeter ID	OSL result, arbitrary units			Mean	Standard deviation	c_v (%)
	Measurement					
	1	2	3			
1	17230	17291	17187	17236	52.2	0.3
2	17058	16785	17043	16962	153.4	0.9
3	17441	17345	17092	17292.6	180.2	1.0
4	16825	16764	16494	16694.3	176.1	1.0
5	16672	16632	16720	16674.6	44.1	0.2
6	16729	16933	16710	16790.6	123.6	0.7
7	13863	13842	13887	13864	22.5	0.2
8	14190	14328	14176	14231.3	84.0	0.6
9	16825	16787	16526	16712.6	162.7	1.0

appropriate statistical quantity, to assess the reproducibility of the irradiator, is the c_v. Given that the most used dosimeter in our department is in the form of pellets, the c_v was obtained for this type and size of detector. The OSL response for each dosimeter used with set 1 with an exposition time of 2 min is shown in Table 4.

The low c_v values confirm the reproducibility of the irradiator, and the low influence in the OSL results. Considering each dosimeter individually, the highest c_v (1.0%) was obtained for dosimeters 3, 4 and 9. Similar values of reproducibility were obtained for sets 2 and 3. Therefore, the highest values of uncertainties in the estimated dose rates are related not only to the irradiator, but also to intrinsic characteristics of the detectors and measurement systems. Although a good reproducibility was obtained, the absorbed dose by the sample due to the manual procedure of source placement may increase the uncertainties, and decrease the reproducibility of the irradiator. To overcome these issues, and also obtain different dose values, the source may be coupled to a step motor.

3.4. Comparison with the values of the calibration certificates

The manufacturer of the applicators used in this study presents high values of uncertainty for the dose rates, in their original certificates of calibration: 20% and 30% for dermatological and ophthalmological applicators, respectively. In this context, uncertainties in the dose rates within this range, for the irradiator system, may be considered adequate. Table 5 shows a comparison between the results obtained in the

Table 5
Comparisons between the techniques used for calibration of irradiator and the results from original certificate.

Set number	Absorbed dose rate (mGy/s)[a]	Difference between film and OSLs (%)	Difference between certificate and film results (%)	Difference between certificate and the OSL technique (%)
	Certificate of manufacturer			
1	21.1 ± 6.3	28.7	7.5	34.1
2	8.9 ± 2.6	26.4	1.9	40.4
3	16.8 ± 3.3	11.6	1.7	27.3

[a] Values on April, 2014 obtained from data originally supplied by the manufacturer.

Table 6
Monte Carlo results for the irradiator wall and thoracic region on the FASH phantom.

Position of dosimeter	*F8 (MeV/Part)	Relative Uncertainty
Irradiator wall	3.08E-09	9.1%
FASH thoracic region	9.53E-10	12.1%

Table 7
Results from Monte Carlo simulation, equivalent dose rate and equivalent dose for organs and body tissues based on the duration of handling.[a]

Organs	*F8 Results (MeV/particle)	Relative Error (%)	Weighting Factor[b]	Equivalent Dose Rate (μSv/min)	Equivalent Dose (μSv)
Red bone-marrow	2.0E-15	4.9	0.12	1.6E-08	9.6E-05
Colon	6.4E-16	1.0	0.12	1.2E-08	7.2E-05
Lung	2.5E-15	1.5	0.12	4.8E-08	2.9E-04
Stomach	3.4E-16	1.4	0.12	6.4E-09	3.8E-05
Breast	5.1E-16	1.8	0.12	4.0E-09	2.4E-05
Adrenals	1.1E-17	6.6	0.01	9.0E-11	5.4E-07
Extrathoracic Region	1.3E-15	1.0	0.01	1.0E-08	6.0E-05
Gall Bladder	3.1E-17	2.5	0.01	2.4E-10	1.4E-06
Heart	1.9E-16	3.0	0.01	1.5E-09	9.0E-06
Kidneys	2.8E-16	2.1	0.01	2.2E-09	1.3E-05
Lymphatic nodes	3.0E-16	1.2	0.01	2.4E-09	1.4E-05
Muscle	7.7E-15	0.6	0.01	6.0E-08	3.6E-04
Pancreas	2.6E-16	2.0	0.01	2.1E-09	1.3E-05
Ovaries	6.9E-18	8.3	0.01	5.5E-11	3.0E-05
Small Intestine	8.3E-16	1.2	0.01	6.5E-09	3.6E-05
Spleen	1.7E-16	2.8	0.01	1.3E-09	7.8E-06
Thymus	2.0E-17	8.1	0.01	1.6E-10	9.6E-07
Uterus	4.7E-17	5.2	0.08	3.7E-10	2.2E-06
Esophagus	2.0E-17	5.4	0.04	1.6E-10	9.6E-07
Liver	2.4E-15	1.2	0.04	1.9E-08	1.1E-04
Thyroid	1.7E-17	8.0	0.04	1.4E-10	8.4E-07
Bone surface	6.1E-16	1.1	0.01	9.7E-10	5.8E-06
Brain	7.2E-16	2.9	0.01	6.0E-09	3.6E-05
Salivary glands	9.0E-17	14.2	0.01	7.0E-10	4.2E-06
Skin	1.0E-07	0.5	0.01	1.6E-01	9.6E+02
			Effective dose (μSv)		**9.6E+00**

[a] The duration of exposure considered was approximately 6000 min per year.
[b] The weighting factor values were based on the ICRP (2007).

SAMARA and the results from the original certificate.

The largest differences were observed between the original certificate and the OSL results. The results from films were similar to those values from the original certificate.

The work by Menon and Sloboda (2000) verified the percentage depth dose for four ophthalmic applicators using radiochromic films. They found that the highest differences between the film results and the manufacturer's values were for doses of approximately 20 Gy. For the present study we have not found large discrepancies between the films and the original certificates; all differences were lower than 10%.

3.5. Evaluation of safety conditions

The experimentally measured conversion factor was 1.59E+08 (μSv/min)/(part/MeV). The Monte Carlo results (*F8 tally) for the irradiator wall, and the thoracic region on the FASH virtual phantom, are presented in Table 6.

Using equation (3), the results with the dosimeter in the thoracic region presented a dose rate of (0.15 ± 0.02) μSv/min, and based on these results, the $Hp_{(10)}$ value can be estimated.

The ICRP (2007) Report recommends yearly individual dose limits of 20 and 1 mSv for IOE and the public, respectively. Assuming that a user may handle the irradiator for approximately 30 min, five times per week, after one year the dose for individuals can be estimated using equation (4) as approximately 1.0 mSv for $Hp_{(10)}$.

Examining the tissues of the body individually, the results of a Monte Carlo simulation are summarized in Table 7. The effective dose values were determined using equation (5).

The results for the dose rates on organs were very low except for the skin, which presented approximately 1.6E-01 μSv/min. The effective dose obtained using equation (5) was 9.6E+00 μSv, during a period of one year. This value is within the recommended limit – 20 mSv (IOE) and 1 mSv (public) (ICRP, 2007). Therefore, these results demonstrate that handling conditions for the prototype irradiator SAMARA are adequate and safe.

4. Conclusions

The methodology presented in this study may provide new functionality to dermatological and ophthalmic radioactive applicators used in beta therapy. Using these applicators, an irradiator can be assembled, and it is easy to handle and supports up to three individual sources for use in research institutions. Although the institution that intends to construct an irradiator of this type may not know the dose rates of these applicators, the use of radiochromic films or OSL dosimeters may determine these values. While the prototype irradiator SAMARA provides safe conditions for handling, all protocols must be followed. In many countries, changing the purpose of a radioactive source may require regulatory approvals that were not addressed in this work. Before the construction of the irradiator, all relevant regulatory documentation must be secured.

Acknowledgments

The authors would like to thank Dr. Richard Kramer for kindly providing the virtual anthropomorphic phantoms. This work was partially supported by the Brazilian agencies: Fundação de Amparo à Pesquisa do Estado de Minas Gerais (FAPEMIG, Grants No. APQ-03049-15 and APQ-02934-15), Fundação de Apoio à Pesquisa e à Inovação Tecnológica do Estado de Sergipe (CAPES/FAPITEC-SE, Grant No. 88881.157892/2017-01) and Conselho Nacional de Desenvolvimento Científico e Tecnológico (CNPq, Grants No. 421603/2016-0, 420699/2016-3, 308090/2016-0 and 427010/2016-0), and PRPGI/IFBA – Instituto Federal da Bahia-Brazil.

References

Abdi, H., 2010. Coefficient of variation. In: Neil, Salkind (Ed.), Encyclopedia of Research Design. Sage, Thousand Oaks, CA.

Akselrod, M.S., McKeever, S.W.S., 1999. Radiation dosimetry method using pulsed optically stimulated luminescence. Radiat. Protect. Dosim. 81, 167–176. https://doi.org/10.1093/oxfordjournals.rpd.a032583.

Altinkaynak, H., Demircan, A., Kocasaraç, C., Kara, N., Dundar, H., Altan, Ç., Demirok, A., 2014. Effect of orbital protrusion and vertical interpalpebral distance on pterygium formation. Contact Lens Anterior Eye 37, 153–156. https://doi.org/10.1016/j.clae.2013.09.010.

Antonio, P.L., Pinto, T.C.N.O., Silva, R.M.V., Souza, D.N., Caldas, L.V.E., 2014. The use of the TL and OSL phenomena for determination of absorbed dose rates of $^{90}Sr+^{90}Y$ sources by a postal method. Radiat. Meas. 71, 305–309. https://doi.org/10.1016/j.radmeas.2014.03.021.

Barouky, J., Fournier-Bidoz, N., Mazal, A., Fares, G., Rosenwald, J.C., 2011. Practical use of Gafchromic® EBT films in electron beams for in-phantom dose distribution measurements and monitor units verification. Phys. Med. 27, 81–88. https://doi.org/10.1016/j.ejmp.2010.04.001.

Briesmeister, J.F., 2000. MCNP - A General Monte Carlo N-Particle Transport Code. Los Alamos National Laboratory.

Cassola, V.F., Lima, V.J.M., Kramer, R., Khoury, H., 2010. FASH and MASH: female and Male adult human phantoms based on polygon mesh surfaces: development of the anatomy. Phys. Med. Biol. 55, 133–162. https://doi.org/10.1088/0031-9155/55/1/009.

Deasy, J.O., Soares, C.G., 1994. Extrapolation chamber measurements of $^{90}Sr+^{90}Y$ beta-particle ophthalmic applicator dose rates. Med. Phys. 21, 91–99. https://doi-org.ez34.periodicos.capes.gov.br/10.1118/1.597239.

Eckerman, K.F., Westfall, R.J., Ryman, J.C., Cristy, M., 1993. DEXRAX32: Decay Data

Extractor. Oak Ridge National Laboratory.
Froelich, K., Staudenmaier, R., Kleinsasser, N., Hagen, R., 2007. Therapy of auricular keloids: review of different treatment modalities and proposal for a therapeutic algorithm. Eur. Arch. Oto-Rhino-Laryngol. 264, 1497–1508. https://doi.org/10.1007/s00405-007-0383-0.
ICRP, 2007. The 2007 recommendations of the international commission on radiological protection. ICRP publication 103. Ann. ICRP 37 (2–4).
International Commission on Radiation Units and Measurements, 1993. Quantities and Units in Radiation Protection Dosimetry. ICRU Report 51. ICRU. . https://doi.org/10.1093/jicru/os26.2.Report51.
Mackenzie, F.D., Hirst, L.W., Kynaston, B., Bain, C., 1991. Recurrence rate and complications after beta irradiation for pterygium. Ophthalmology 98, 1776–1780. https://doi.org/10.1016/S0161-6420(91)32051-7.
Menon, G., Sloboda, R., 2000. Measurement of relative output factor for 90Sr ophthalmic applicators using radiochromic film. Med. Dosim. 25, 171–177. https://doi.org/10.1016/S0958-3947(00)00045-5.
Santos, W.S., Carvalho, A.B., Hunt, J.G., Maia, A.F., 2013. Using the Monte Carlo technique to calculate dose conversion coefficients for medical professionals in interventional radiology. Radiat. Phys. Chem. 95, 177–180. https://doi.org/10.1016/j.radphyschem.2013.01.036.
Su, F.-C., Liu, Y., Stathakis, S., Shi, C., Esquivel, C., Papanikolaou, N., 2007. Dosimetry characteristics of GAFCHROMIC® EBT film responding to therapeutic electron beams. Appl. Radiat. Isot. 65, 1187–1192. https://doi.org/10.1016/j.apradiso.2007.05.005.
Wilcox, E.E., Daskalov, G., 2007. Evaluation of gafchromic EBT film for cyberknife dosimetry. Med. Phys. 34, 1967–1974. https://doi-org.ez34.periodicos.capes.gov.br/10.1118/1.2734384.
Willner, J., Flentje, M., Lieb, W., 2001. Soft x-ray therapy of recurrent pterygium an alternative to ^{90}Sr eye applicators. Strahlenther. Onkol. 177, 404–409. https://doi.org/10.1007/PL00002422.
Yukihara, E.G., McKeever, S.W.S., 2008. Optically stimulated luminescence (OSL) dosimetry in medicine. Phys. Med. Biol. 53, 351–379. https://doi.org/10.1088/0031-9155/53/20/R01.